



Rabbit 3-hydroxyhexobarbital dehydrogenase is a NADPH-preferring reductase with broad substrate specificity for ketosteroids, prostaglandin D₂, and other endogenous and xenobiotic carbonyl compounds



Satoshi Endo^{a,*}, Toshiyuki Matsunaga^a, Atsuko Matsumoto^a, Yuki Arai^a, Satoshi Ohno^b, Ossama El-Kabbani^c, Kazuo Tajima^d, Yasuo Bunai^e, Shigeru Yamano^f, Akira Hara^{b,e}, Yukio Kitade^b

^a Gifu Pharmaceutical University, Gifu 502-1196, Japan

^b Faculty of Engineering, Gifu University, Gifu 501-1193, Japan

^c Victorian College of Pharmacy, Monash University, Parkville, Victoria 3052, Australia

^d Faculty of Pharmaceutical Sciences, Hokuriku University, Kanazawa 920-1181, Japan

^e Graduate School of Medicine, Gifu University, Gifu 501-1193, Japan

^f Faculty of Pharmaceutical Sciences, Fukuoka University, Fukuoka 814-0180, Japan

ARTICLE INFO

Article history:

Received 27 June 2013

Accepted 14 August 2013

Available online 27 August 2013

Keywords:

Aldo-keto reductase

Ketosteroid reductase

3-Hydroxyhexobarbital dehydrogenase

4-Oxo-2-nonenal

Prostaglandin D₂

ABSTRACT

3-Hydroxyhexobarbital dehydrogenase (3HBD) catalyzes NAD(P)⁺-linked oxidation of 3-hydroxyhexobarbital into 3-oxohexobarbital. The enzyme has been thought to act as a dehydrogenase for xenobiotic alcohols and some hydroxysteroids, but its physiological function remains unknown. We have purified rabbit 3HBD, isolated its cDNA, and examined its specificity for coenzymes and substrates, reaction directionality and tissue distribution. 3HBD is a member (AKR1C29) of the aldo-keto reductase (AKR) superfamily, and exhibited high preference for NADP(H) over NAD(H) at a physiological pH of 7.4. In the NADPH-linked reduction, 3HBD showed broad substrate specificity for a variety of quinones, ketones and aldehydes, including 3-, 17- and 20-ketosteroids and prostaglandin D₂, which were converted to 3 α -, 17 β - and 20 α -hydroxysteroids and 9 α ,11 β -prostaglandin F₂, respectively. Especially, α -diketones (such as isatin and diacetyl) and lipid peroxidation-derived aldehydes (such as 4-oxo- and 4-hydroxy-2-nonenals) were excellent substrates showing low *K_m* values (0.1–5.9 μ M). In 3HBD-overexpressed cells, 3-oxohexobarbital and 5 β -androstan-3 α -ol-17-one were metabolized into 3-hydroxyhexobarbital and 5 β -androstane-3 α ,17 β -diol, respectively, but the reverse reactions did not proceed. The overexpression of the enzyme in the cells decreased the cytotoxicity of 4-oxo-2-nonenal. The mRNA for 3HBD was ubiquitously expressed in rabbit tissues. The results suggest that 3HBD is an NADPH-preferring reductase, and plays roles in the metabolisms of steroids, prostaglandin D₂, carbohydrates and xenobiotics, as well as a defense system, protecting against reactive carbonyl compounds.

© 2013 Elsevier Inc. All rights reserved.

1. Introduction

Hexobarbital, a short time-acting hypnotic, is metabolized to 3-hydroxyhexobarbital (3HB) by cytochrome P450, and then

Abbreviations: 3HB, 3-hydroxyhexobarbital; 3OB, 3-oxohexobarbital; 3HBD, 3-hydroxyhexobarbital dehydrogenase; AKR, aldo-keto reductase; HSD, hydroxysteroid dehydrogenase; PG, prostaglandin; TBE, 6-*tert*-butyl-2,3-epoxy-5-cyclohexene-1,4-dione; 4R-TBEH, 6-*tert*-butyl-2,3-epoxy-4(*R*)-hydroxy-5-cyclohexen-1-one; RT, reverse transcription; BAEC, bovine aortic endothelial cell; LC-ESI-MS, liquid chromatography–electrospray ionization–mass spectrometry.

* Corresponding author at: Laboratory of Biochemistry, Gifu Pharmaceutical University, Gifu 501-1196, Japan. Tel.: +81 58 230 8100; fax: +81 58 230 8105.

E-mail address: sendo@gifu-pu.ac.jp (S. Endo).

to 3-oxohexobarbital (3OB) by 3-hydroxyhexobarbital dehydrogenase (3HBD) (Fig. 1) [1,2]. While 3HB is excreted after conjugation with glucuronic acid, electrophilic 3OB reacts with glutathione to produce 1,5-dimethylbarbituric acid and cyclohexenone–glutathione adduct [3,4]. Because 3HBD is involved in the formation of the reactive 3OB as well as the hexobarbital metabolism, it has been purified and characterized from liver cytosols of rabbits [5–7], guinea-pigs [8,9], mice [10] and golden hamsters [11]. The enzymes are monomeric proteins with molecular weights of 31–42 kDa, and oxidize several other alicyclic alcohols including some 3 α - and/or 17 β -hydroxysteroids in the presence of either NAD⁺ or NADP⁺ as the coenzyme. However, they differ from one another in their reactivity toward the substrates. In the reactivity toward the α - and β -isomers of 3HB (α -3HB and β -3HB,

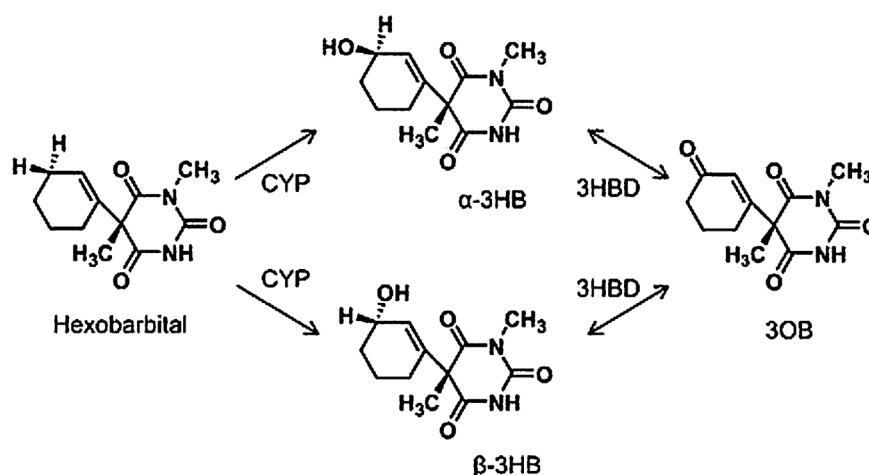


Fig. 1. Metabolism of hexobarbital into 3HB and 3OB. Hexobarbital is oxidized by cytochrome P450 (CYP) into α - and β -isomers of 3HB, which are converted into 3OB by 3HBD. The structures of (+)-hexobarbital and its metabolites are shown.

respectively, Fig. 1), all the enzymes oxidize α -3HB more preferentially than β -3HB, but the activities of the mouse and hamster enzymes toward β -3HB are much lower compared to those of the other animal enzymes. The mouse and hamster enzymes also oxidize *trans*-benzene dihydrodiol that is a representative substrate of dihydrodiol dehydrogenase [10,11]. Guinea-pig 3HBD is distinguishable from the other animal enzymes in its low activity for other xenobiotic alicyclic alcohols (such as 1-indanol and 1-tetralol) and high activity for 17 β -hydroxy-C₁₉-steroids, thereby suggesting its identity with testosterone 17 β -dehydrogenase (EC. 1.1.1.64) [8,9]. The mouse enzyme also exhibits 17 β -hydroxysteroid dehydrogenase (HSD) activity for 17 β -hydroxy-C₁₉-steroids and 17 β -estradiol [10] that is not the substrate for the guinea-pig enzyme [8]. The rabbit enzyme oxidizes limited 17 β -hydroxysteroids such as 5 β -androstane-3 α ,17 β -diol [7]. The hamster enzyme exhibits 3 α -HSD activity toward bile acids, in addition to the 17 β -HSD activity for 5 β -androstane-3 α ,17 β -diol [11]. The enzymatic properties of mammalian 3HBDs were studied under optimal pH conditions of 8.0–10.5, where their NAD⁺-linked dehydrogenase activities are higher than the NADP⁺-linked activities. Therefore, 3HBD has been reported to act as a dehydrogenase for the above xenobiotic and steroidal alcohols, but its physiological role has not yet been clarified. Among the mammalian 3HBDs, only hamster 3HBD is so far molecularly cloned and shown to be a member of the aldo-keto reductase (AKR) superfamily [11]. This suggests a possibility that the mammalian enzymes reduce carbonyl compounds, but their substrate specificities in the reduction reaction have not yet been thoroughly characterized.

In rabbits, hepatic 3HBD was reported to be identical to indanol dehydrogenase [6]. In contrast, six multiple forms of indanol dehydrogenase associated with 17 β -HSD activity are isolated from the liver cytosol [12]. In addition, cytosolic 17 β -HSD [13,14] and dihydrodiol dehydrogenase with 17 β -HSD activity [15] exist in multiple forms in rabbit liver. Furthermore, the recent rabbit genomic analysis has predicted several genes that encode HSD-like proteins belonging to the AKR1C subfamily, three of which have recently been identified as NAD⁺-preferring 3 α /17 β -HSDs (AKR1C26–AKR1C28) [16]. In this study, we isolated the cDNA for rabbit 3HBD that has been assigned AKR1C29 in the AKR superfamily. To elucidate the physiological role of AKR1C29 and its functional relationship with the enzymes that metabolize steroids and xenobiotic alcohols, we characterized the properties of the recombinant AKR1C29 at a physiological pH of 7.4, and examined

the metabolism of the substrates in the enzyme-overexpressed cells. Our data show that AKR1C29 acts as a NADPH-preferring reductase with a wide range of both aromatic and aliphatic carbonyl compounds including ketosteroids, prostaglandin (PG) D₂ and lipid peroxidation-derived aldehydes.

2. Materials and methods

2.1. Chemicals

Steroids were obtained from Sigma Chemicals (Perth, WA) and Steraloids (Newport, RI), and PGs, 4-oxo-2-nonenal and 4-hydroxy-2-nonenal were from Cayman Chemicals (Ann Arbor, MI). 3OB [5], *trans*-benzene dihydrodiol [17], 4-oxo-2-nonenol [18] geranylgeraniol [19], 6 α / β -naloxols [20,21], 6-*tert*-butyl-2,3-epoxy-5-cyclohexene-1,4-dione (TBE) [22], 6-*tert*-butyl-2,3-epoxy-4(*R*)-hydroxy-5-cyclohexen-1-one (4*R*-TBEH) and its 4*S*-isomer (4*S*-TBEH) [23] were synthesized as described previously. α - and β -3HBs were kindly denoted by Dr R. Takenoshita (Fukuoka University, Japan). 3-Deoxyglucosone and befunolol were gifts from Nippon Zoki Pharmaceutical Co. (Osaka, Japan) and Kaken Pharmaceutical Co. (Tokyo, Japan), respectively. All other chemicals were of the highest grade that could be obtained commercially.

2.2. cDNA isolation and RT-PCR analysis

A cDNA for AKR1C29 was isolated from a total RNA sample of small intestine of a Japanese white rabbit by reverse transcription (RT)-PCR. The preparation of total RNA, RT, and DNA techniques followed the standard procedures described by Sambrook et al. [24]. The PCR was performed using *Pfu* DNA polymerase (Agilent Technologies, Santa Clara, CA) and a pair of sense and antisense primers, 5'-ttttcatatgatggatccaagcatcagcgttatgggcatt-3' and 5'-ttttgctcgaactcaatattcatcagaaaatgggtaattt-3', which contain underlined *Nde*I and *Sall* sites, respectively. PCR amplification consisted of an initial denaturation step at 94 °C for 5 min, 29 cycles of denaturation (94 °C/30 s), annealing (60 °C/30 s) and extension (72 °C/2 min), and a final incubation step at 72 °C for 5 min. The PCR products were purified, digested with the two restriction enzymes (Life Technologies, Carlsbad, CA), and ligated into the pCold I vectors (Takara Bio Inc., Otsu, Japan) that had been digested with the two restriction enzymes [25]. The sequence of the coding region of the cloned cDNA was analyzed using a Beckman Coulter CEQ8000XL DNA sequencer. The 972-base pair sequence of the

cDNA was deposited in DDBJ database with the accession number AB821295.

In the RT-PCR analysis of the expression of mRNA for AKR1C29 in rabbit tissues, the preparation of total RNA samples, RT and PCR were carried out as described above. The cDNA for rabbit β -actin was also amplified as an internal control with a pair of sense and antisense primers, 5'-ccggcttcgaggcgacg-3' and 5'-tccggcgaccgaggtcc-3', respectively. The PCR products were separated by agarose gel electrophoresis, and revealed with ethidium bromide.

2.3. Enzyme purification

The expression construct was transfected into *Escherichia coli* BL21 (DE3) pLysS, and the recombinant AKR1C29 fused to the N-terminal 6-His tag was expressed and purified to homogeneity from the cell extracts using the nickel-charged Sepharose 6FF resin (GE Healthcare, Chalfont St Giles, UK) as described previously [25]. 3HBD was purified to homogeneity from the rabbit liver (50 g) by the methods of Takenoshita and Toki [5], except that Q-Sepharose (GE Healthcare) was used instead of TEAE-cellulose. The protein concentrations of the enzymes were determined with Bradford reagent using bovine serum albumin as the standard.

2.4. Mass spectrometry

The identity of the purified hepatic 3HBD with AKR1C29 was examined by the mass spectrometry method. The purified protein (0.1 mg) was digested by lysylendopeptidase, and then the digest was analyzed using a Bruker-Franzen Mass Spectrometry System Ultraflex TOF/TOF with a saturated α -cyano-4-hydroxycinnamic acid matrix as described previously [26].

2.5. Assay of enzyme activity

The dehydrogenase activities for the enzymes were assayed by measuring the rate of change in fluorescence (at 455 nm with an excitation wavelength of 340 nm) or absorbance (at 340 nm) of NAD(P)H. The corresponding standard reaction mixture consisted of 0.1-M potassium phosphate buffer, pH 7.4, 0.25-mM NADP⁺ or 2.0-mM NAD⁺, substrate and enzyme, in a total volume of 2.0 mL. The reductase activities, except for all-*trans*-retinal reductase activity, were determined by measuring the rate of change in NAD(P)H absorbance in the phosphate buffer, pH 7.4, containing 0.1-mM NADH or NADPH and an appropriate amount of carbonyl substrate. The assay of all-*trans*-retinal reductase activity was performed according to the method of Parés and Julià [27], except that 0.1-M potassium phosphate, pH 7.4, containing 0.01% Tween 80 was added as the buffer. One unit of enzyme activity was defined as the amount of enzyme that catalyzes the formation or oxidation of 1 μ mol NAD(P)H per min at 25 °C.

The apparent K_m and k_{cat} values for coenzymes and substrates were determined by fitting the initial velocities to the Michaelis–Menten equation. The IC_{50} values for inhibitors were determined with 2- μ M β -ionol as the substrate in the above standard reaction mixture. The inhibitor constant, K_i , was estimated from the Dixon plot and/or Cornish–Bowden plot of the velocities obtained in the β -ionol range (0.5–20 $\times K_m$) with three concentrations of the inhibitor. The kinetic constants and IC_{50} values are expressed as the means of at least three determinations. The standard deviations of the determinations were less than 15%, unless otherwise noted.

2.6. Product identification

The reaction was conducted at 37 °C in a 2.0-mL reaction mixture, containing coenzyme (1-mM NADP⁺ or 0.1-mM NADPH), substrate (0.05–0.1 mM), enzyme (0.1–0.3 mg), and

0.1-M potassium phosphate, pH 7.4. The substrate and products were extracted into 4-mL ethyl acetate 30 min after the reaction was started at 37 °C. The products of oxidoreduction of steroids [25] and reduction of PGD₂ [28], farnesal [29] and 4-oxo-2-nonenal [18] were analyzed by TLC, as described. The reduced products of TBE were identified by the HPLC methods [23]. The products of 3HB oxidation, 3OB reduction, 5 β -androstane-3 α ,17 β -diol oxidation and 5 β -androstane-3 α -ol-17-one reduction were analyzed by the liquid chromatography–electrospray ionization–mass spectrometry (LC–ESI–MS) using a Hewlett-Packard HP 1100 Series LC/MSD system attached with a diode array detector and a column (Mightysil RP-18 GP 5 μ m, 4.6 mm \times 250 mm, Kanto Chemical Co., Tokyo, Japan). Separations were carried out at a flow rate of 0.5 mL/min and 40 °C using the following mobile phases: 25% acetonitrile aqueous solution containing 0.1% formic acid for 3OB and α/β -3HBs, and 80% acetonitrile aqueous solution containing 0.1% formic acid for the two steroids. 3OB, α -3HB, β -3HB, 5 β -androstane-3 α -ol-17-one and 5 β -androstane-3 α ,17 β -diol were detected by monitoring their total ions (m/z 249.1, 251.1, 251.1, 289.4 and 291.4, respectively) in the negative ESI mode, and eluted at the retention times of 20.1, 17.6, 16.8, 14.9 and 12.7 min, respectively. The detection limits of 3OB, α/β -3HBs and the two steroids were 0.1, 0.1 and 1 nmol, respectively.

2.7. Cell culture experiments

Bovine aortic endothelial cells (BAECs) were generous gift from Taisho Pharmaceutical Co. (Saitama, Japan), and cultured in Dulbecco's modified Eagle medium supplemented with 10% fetal bovine serum, penicillin (100 units/mL) and streptomycin (0.1 mg/mL) at 37 °C in a humidified incubator containing 5% CO₂. The construction and transfection of the pGW1 plasmids harboring the cDNA for AKR1C29 into BAECs were performed as described previously [30]. Briefly, the cDNA was amplified by PCR using the primers. The sense primer, 5'-ccccgaattcGCCACCatgatccaagcatcagcg-3', contains an *Eco*RI site, a Kozak sequence and a start codon, which are shown in underlined, capital and italic letters, respectively. The antisense primer was the same as that used for the cDNA cloning. After the sequences of the PCR products were verified, they were subcloned at the *Eco*RI and *Sall* sites of the pGW1 expression vector. Using a Lipofectamine 2000 reagent (Life Technologies), the cells were transfected with the expression plasmids. The transfected cells were maintained in the medium (2 mL) containing 2% fetal bovine serum for 24 h, and then incubated with α -3HB, 3OB (each 200 μ M), 5 β -androstane-3 α -ol-17-one or 5 β -androstane-3 α ,17 β -diol (each 100 μ M) at different times. The culture medium was collected by centrifugation, and the lipidic fraction of the medium was extracted twice by 4-mL ethyl acetate. The extract was evaporated to dryness, and the residue was dissolved in methanol (0.1 mL). The portion (10 μ L) of the sample was analyzed by the LC–ESI–MS method as described above. The amounts of the eluted substrates and metabolites were quantified from their peak areas using the standard curves constructed with the authentic samples. The effects of the AKR1C29 overexpression on the cytotoxicity of 4-oxo-2-nonenal were examined using the above BAECs as described previously [25].

3. Results

3.1. Amino acid sequence and cDNA cloning of 3HBD

3HBD was purified from rabbit liver and its 13 lysylendopeptidase-digested peptides were subjected to amino acid sequence analysis by the mass spectrometry (Fig. 2). The sequences

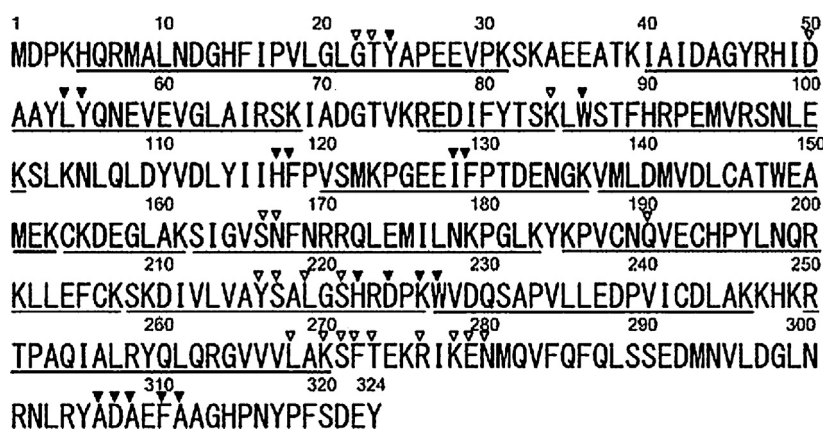


Fig. 2. Amino acid sequence of AKR1C29. The underlined residues are identical to those determined by peptide sequencing of rabbit liver 3HBD. The NAD(P)(H)- and substrate-binding residues of the structurally evaluated AKR1C subfamily enzymes [33,39–42] are shown by open and closed arrowheads, respectively.

(composed of a total 213 residues) coincided with that of an *Oryctolagus cuniculus* PGE₂ 9-reductase like protein (NCBI accession no. XP_002721727.1) among the AKR1C subfamily proteins predicted from the rabbit genomic analysis. This protein has been assigned as AKR1C29 in the AKR superfamily. The cDNA for AKR1C29 was cloned by RT-PCR, and its nucleotide sequence was identical to that predicted from the genomic analysis, with the exception of two nucleotide replacements (⁸⁴⁷A → C and ⁸⁵⁵C → T) that cause one amino acid replacement (Phe283 → Val) in the predicted sequence.

The purified recombinant AKR1C29 showed both NAD⁺- and NADP⁺-linked dehydrogenase activities toward α-3HB and (S)-1-tetralol, and the pH optima of the NAD⁺- and NADP⁺-linked activities were 9.5 and 10.5, respectively, as described previously with hepatic 3HBD [5]. The *K_m* and *k_{cat}* values for α-3HB determined in 0.1-M glycine–NaOH buffer, pH 9.5, containing 1.0-mM NAD⁺ were 0.19 mM and 528 min⁻¹, respectively, which are also comparable to those reported with hepatic 3HBD [5]. AKR1C29 exhibited NADH- and NADPH-linked reductase activities toward pyridine-3-aldehyde, which showed similar pH optima at 6.0. Therefore, the enzymatic properties of AKR1C29 were examined at a physiological pH of 7.4, in order to compare the kinetic constants for the coenzymes and substrates between the oxidation and reduction reactions.

3.2. Coenzyme specificity

When the (S)-1-tetralol dehydrogenase and pyridine-3-aldehyde reductase activities of AKR1C29 were assayed in 0.1-M Tris–HCl buffer (pH 7.4), the NAD⁺- and NADH-linked activities were much lower than those determined in 0.1-M potassium phosphate buffer (pH 7.4), but the NADP⁺- and NADPH-linked activities were independent of the buffer component (Fig. 3). The NAD(H)-linked activities in the Tris–HCl buffer were enhanced in a dose-dependent manner (from 0 to 80 mM) by the addition of the phosphate buffer, and reached the activity level determined in 0.1-M phosphate buffer. As observed with guinea-pig 3HBD [9], phosphate ion also acted as an activator of the NAD(H)-linked activities of AKR1C29. The kinetic constants for the coenzymes and (S)-1-tetralol determined with the phosphate and Tris–HCl buffers are summarized in Table 1. In the phosphate buffer, both *K_m* and *k_{cat}* values for NAD(H) were higher than those for NADP(H), but the *k_{cat}*/*K_m* values indicated approximately 22- and 5-fold preferences for NADP(H) over NAD(H) in the oxidation and reduction reactions, respectively. In the Tris–HCl buffer, the preferences for NADP(H) over NAD(H) were much greater mostly due to the 3-fold decrease in *k_{cat}* values of the NAD(H)-linked activities, compared to the

values determined in the phosphate buffer. The difference in *k_{cat}*/*K_m* values for (S)-1-tetralol between the NAD⁺- and NADP⁺-linked activities was low compared to that for the coenzymes.

In order to confirm the preferences for NADP(H) over NAD(H), we compared the inhibitory effects of NAD⁺ and NADP⁺ on the NADH- and NADPH-linked reductase activities in the phosphate buffer (Table 2). The NADH-linked activity was potently inhibited by NADP⁺ in contrast to low inhibition by NAD⁺, whereas the NADPH-linked activity was weakly inhibited by NADP⁺ and hardly affected by the addition of NAD⁺. In the 0.1-mM NAD(P)⁺-linked reverse reaction with α-3HB as the substrate, NADPH inhibited the NAD⁺-linked activity more potently than the NADP⁺-linked activity, while 0.1-mM NADH showed less than 24% inhibition toward the NAD(P)⁺-linked activity. The inhibition pattern of NADPH was competitive with respect to NAD⁺, showing the *K_i* value of 0.10 μM. The potent inhibition of NAD(H)-linked activity

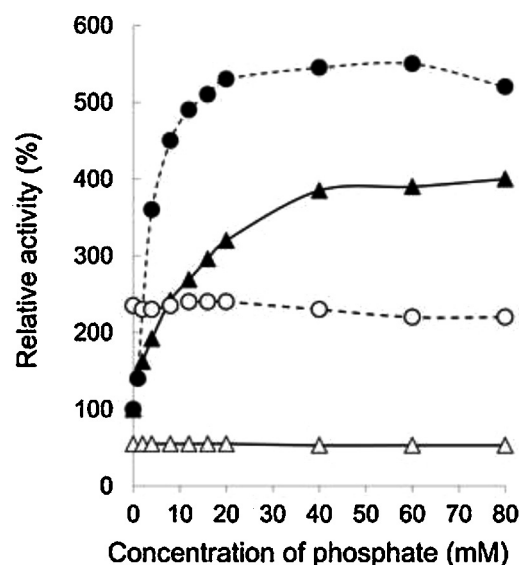


Fig. 3. Effect of phosphate on the NAD(H)- and NADP(H)-linked activities of AKR1C29. The enzyme activities were determined in 0.1-M Tris–HCl buffer, pH 7.4, in the absence or presence of indicated concentrations of potassium phosphate buffer, pH 7.4. The substrate and coenzyme for the dehydrogenase activity (solid line) were 0.1-mM (S)-1-tetralol and 2.0-mM NAD⁺ (▲) or 0.25-mM NADP⁺ (△), respectively and those for the reductase activity (dotted line) were 2.0-mM pyridine-3-aldehyde and 0.1-mM NADH (●) or NADPH (○). The activities are expressed as relative activities (means of two determinations), in which the NAD⁺-linked dehydrogenase and NADH-linked reductase activities in the absence of the phosphate buffer are taken as 100%.

Table 1
Kinetic constants for coenzymes and substrates in the oxidation and reduction reactions by AKR1C29.

Varied substrate	Fixed substrate	Phosphate buffer			Tris-HCl buffer		
		K_m (μM)	k_{cat} (min^{-1})	k_{cat}/K_m ($\text{min}^{-1} \mu\text{M}^{-1}$)	K_m (μM)	k_{cat} (min^{-1})	k_{cat}/K_m ($\text{min}^{-1} \mu\text{M}^{-1}$)
Oxidation							
NAD ⁺	1-mM (S)-1-Tetralol	471	111	0.24	454	34	0.075
NADP ⁺	0.1-mM (S)-1-Tetralol	1.6 (0.003)	8.4 (0.08)	5.3 (22)	1.2 (0.003)	7.9 (0.2)	6.6 (88)
(S)-1-Tetralol	2-mM NAD ⁺	12	101	8.4	29	39	1.3
(S)-1-Tetralol	0.25-mM NADP ⁺	1.0 (0.08)	8.5 (0.08)	8.5 (1)	0.9 (0.03)	10 (0.3)	11 (8)
Reduction							
NADH	2-mM P3A ^a	25	17	0.68	13	2.6	0.20
NADPH	2-mM P3A ^a	1.5 (0.06)	5.0 (0.3)	3.3 (5)	1.0 (0.08)	5.2 (2)	5.2 (26)

The activity was assayed in 0.1-M potassium phosphate buffer or Tris-HCl buffer (pH 7.4). The value in parenthesis represents the ratio of the NAD(P)(H)-linked activity to the NAD(H)-linked activity.

^a Pyridine-3-aldehyde.

Table 2
Inhibitory effects of coenzymes on NAD(P)H-linked reductase and NAD(P)⁺-linked dehydrogenase activities of AKR1C29.

Pyridine-3-aldehyde reductase activity	IC_{50} (μM)		α -3HB dehydrogenase activity	IC_{50} (μM)	
	NADP ⁺	NAD ⁺		NADPH	NADH
NADH-linked	0.3	310	NAD ⁺ -linked	0.4	(24%)
NADPH-linked	212	(12%)	NADP ⁺ -linked	47	(20%)

The activities were determined with 0.1 mM coenzyme and 2-mM pyridine-3-aldehyde or 0.5-mM α -3HB. The values in parentheses represent the inhibition percentages by 1 mM NAD⁺ and 0.1 mM NADH.

by NADP(H) further indicates that AKR1C29, i.e., 3HBD, is a NADP(H)-preferring enzyme. Therefore, the substrate specificity of the enzyme was examined with NADP(H) as the coenzyme in 0.1-M phosphate buffer, pH 7.4.

3.3. Substrate specificity

3.3.1. Substrates in NADP⁺-linked oxidation

AKR1C29 oxidized α -3HB more efficiently than its isomer β -3HB (Table 3), as previously determined at the optimal pH of 9.5 with hepatic 3HBD [5]. The enzyme showed high activity toward the known 3HBD substrates such as 1-tetralol and 1-indanol [5,7], in which high preferences for their (S)-isomers over (R)-isomers were observed. The enzyme showed low activity toward other alicyclic alcohols including endogenous $9\alpha,11\beta$ -PGF₂, but did not oxidize 0.1 mM PGF_{2 α} and $9\beta,11\alpha$ -PGF₂, suggesting its specific oxidation of 11β -hydroxy group of PGF₂. AKR1C29 also oxidized several aliphatic alcohols including the most efficient substrate β -ionol showing the highest k_{cat}/K_m value of $12 \text{ min}^{-1} \mu\text{M}^{-1}$, although no activity was observed with sugar alcohols (glycerol, L-threitol and xylitol). Furthermore, AKR1C29 oxidized not only 17β -hydroxysteroids, but also some 3α - and 20α -hydroxysteroids. The oxidized products of $5\alpha/\beta$ -androstane- $3\alpha,17\beta$ -diols were identified as their 17-keto metabolites, and the oxidation of $5\alpha/\beta$ -pregnane- $3\alpha,20\alpha$ -diols yielded $5\alpha/\beta$ -pregnan- 3α -ol- 20 -ones. AKR1C29 did not show significant activity toward other 3α -hydroxysteroids (5β -androstan- 3α -ol- 17 -one, $5\alpha/\beta$ -pregnan- 3α -ol- 20 -ones, 4-pregnen- 3α -ol- 20 -one and lithocholic acid) and 20α -hydroxysteroids ($5\alpha/\beta$ -pregnan- 20α -ol- 3 -ones and 4-pregnen- 20α -ol- 3 -one). The enzyme showed low activity (0.003 unit/mg) toward $50 \mu\text{M}$ 5α -androstan- 3β -ol- 17 -one, but did not oxidize other 3β -hydroxysteroids (5β -androstan- 3β -ol- 17 -one, $5\alpha/\beta$ -pregnan- 3β -ol- 20 -ones and isolithocholic acid). In addition, no activity was observed with the following substrates: 17α -hydroxysteroids ($5\alpha/\beta$ -androstan- 17α -ol- 3 -one and 17α -estradiol), 20β -hydroxysteroids ($5\alpha/\beta$ -pregnan- 20β -ol- 3 -ones and 4-pregnen- 20β -ol- 3 -one), and 21 -hydroxysteroids ($5\alpha/\beta$ -pregnane- 21 -ol- $3,20$ -diones and 11 -deoxycorticosterone).

3.3.2. Substrates in the NADPH-linked reduction

AKR1C29 showed extremely broad substrate specificity for a variety of ketosteroids (Table 4), quinones, ketones (Table 5), dicarbonyl compounds (Table 6), aldehydes and several monosaccharides (Table 7). The enzyme reduced 3-, 17- and 20-ketosteroids

Table 3
Kinetic constants for substrates in the NADP⁺-linked oxidation by AKR1C29.

Substrate	K_m (μM)	k_{cat} (min^{-1})	k_{cat}/K_m ($\text{min}^{-1} \mu\text{M}^{-1}$)
Alicyclic alcohols			
(S)-1-Tetralol	1.0	7.5	7.5
1-Acenaphthenol	8.2	18	2.2
α -3HB	5.0	11	2.2
(S)-1-Indanol	9.8	12	1.2
β -3HB	16	8.4	0.53
<i>trans</i> -Benzene dihydrodiol	12	4.0	0.33
$9\alpha,11\beta$ -PGF ₂	33	0.45	0.014
(R)-1-Indanol	512	1.6	0.003
(R)-1-Tetralol	488	1.1	0.002
Aliphatic alcohols			
β -Ionol	0.2	2.5	12
Geraniol	5.4	1.9	0.35
Farnesol	2.0	0.16	0.080
1-Decanol	4.2	0.33	0.079
Geranylgeraniol	3.8	0.23	0.061
1-Nonanol	537	1.0	0.002
3α-Hydroxysteroids			
4-Androsten- 3α -ol- 17 -one	1.2	0.31	0.26
5α -Androstan- 3α -ol- 17 -one	2.4	0.15	0.063
17β-Hydroxysteroids			
5β -Androstane- $3\alpha,17\beta$ -diol	7.2	2.8	0.35
5α -Androstane- $3\alpha,17\beta$ -diol	1.8	0.49	0.27
5β -Androstan- 17β -ol- 3 -one	4.8	1.3	0.27
5α -Androstan- 17β -ol- 3 -one	1.8	0.47	0.26
5β -Androstane- $3\beta,17\beta$ -diol	7.0	1.1	0.16
5α -Androstane- $3\beta,17\beta$ -diol	12	0.67	0.056
Testosterone	10	0.39	0.039
20α-Hydroxysteroids			
4-Pregnene- $17\alpha,20\alpha$ -diol- 3 -one	2.9	0.26	0.090
5α -Pregnane- $3\alpha,20\alpha$ -diol	35	0.60	0.017
5β -Pregnane- $3\alpha,20\alpha$ -diol	8.3	0.13	0.016

Table 4
Kinetic constants for ketosteroids in the NADPH-linked reduction by AKR1C29.

Substrate	K_m (μM)	k_{cat} (min^{-1})	k_{cat}/K_m ($\text{min}^{-1}\mu\text{M}^{-1}$)
3-Ketosteroids			
5 β -Pregnan-20 α -ol-3-one	1.0	0.70 ^a	0.70
5 α -Pregnan-20 α -ol-3-one	1.9	1.2 ^a	0.63
5 β -Androstan-17 β -ol-3-one	2.3	0.93 ^a	0.40
5 α -Androstan-17 β -ol-3-one	3.7	0.83 ^a	0.22
4-Pregnen-20 α -ol-3-one	16	0.89	0.056
17-Ketosteroids			
5 β -Androstan-3 α -ol-17-one	0.9	2.4	2.7
5 β -Androstan-3 β -ol-17-one	0.9	1.5	1.7
5 α -Androstan-3 α -ol-17-one	14	3.4	0.24
5 α -Androstan-3 β -ol-17-one	11	2.0	0.18
3,17-Diketosteroids			
5 β -Androstane-3,17-dione	1.2	0.86	0.72
5 α -Androstane-3,17-dione	3.6	0.93	0.26
4-Androstene-3,17-dione	13	1.2	0.092
20-Ketosteroids			
5 β -Pregnane-3 α ,21-diol-20-one	0.5	0.59 ^a	1.2
5 α -Pregnane-3 α ,21-diol-20-one	0.9	0.83	0.92
4-Pregnen-3 α -ol-20-one	2.1	1.3	0.62
5 α -Pregnan-3 α -ol-20-one	0.7	0.34 ^a	0.49
5 β -Pregnan-3 α -ol-20-one	1.1	0.39	0.35
3,20-Diketosteroids			
5 α -Pregnane-3,20-dione	0.7	0.72 ^a	1.0
5 β -Pregnane-21-ol-3,20-dione	3.0	2.1	0.70
5 β -Pregnan-3,20-dione	1.4	0.84	0.60
Progesterone	1.1	0.56 ^a	0.51
4-Pregnene-21-ol-3,11,20-trione	1.7	0.80	0.47
5 α -Pregnane-21-ol-3,20-dione	4.5	1.1 ^a	0.24

^a Substrate inhibition was observed at concentrations of $>5 \times K_m$.

Table 5
Kinetic constants for quinones and ketones in the NADPH-linked reduction.

Substrate	K_m (μM)	k_{cat} (min^{-1})	k_{cat}/K_m ($\text{min}^{-1}\mu\text{M}^{-1}$)
p-Quinones			
TBE	0.7	6.7	9.1
1,4-Naphthoquinone	1.5	4.5	3.0
Menadione	0.5	1.3	2.4
Drug ketones			
3OB	3.8	2.1	0.55
Naloxone	16	0.65	0.043
Naltrexone	24	0.94	0.039
Befunolol	424	15	0.035
Daunorubicin	67	1.6	0.024
Haloperidol	55	0.67	0.012
Loxoprofen	272	2.1	0.008
Other ketones			
4-Nitroacetophenone	2.9	4.1	1.4
α -Tetralone	2.8	2.6	0.93
Cyclohexanone	2.4	1.4	0.58
PGD ₂	4.1	0.94	0.23
2-Cyclohexen-1-one	17	3.4	0.20
Acetoin	33	2.9	0.088
4-Benzoylpyridine	56	2.2	0.039
Acetol	35	1.2	0.034

with K_m values in the micromolar or submicromolar range (Table 4). In the 3-ketosteroids, both 5 α - and 5 β -dihydro-C₁₉/C₂₁-steroids were similarly reduced, although substrate inhibition was observed at concentrations higher than $5 \times K_m$. In contrast, the enzyme showed a high K_m value for 4-pregnen-20 α -ol-3-one, and did not reduce testosterone and 5 β -dihydro-C₂₇-steroids (dehydrocholic acid and dehydrolithocholic acid). The reduced products of 5 α / β -pregnan-20 α -ol-3-ones and 5 α / β -pregnan-20 α -ol-3-ones were identified as the corresponding 3 α -ol metabolites. In the 17-

Table 6
Kinetic constants for dicarbonyl compounds in the NADPH-linked reduction.

Substrate	K_m (μM)	k_{cat} (min^{-1})	k_{cat}/K_m ($\text{min}^{-1}\mu\text{M}^{-1}$)
α-Diketones			
9,10-Phenanthrenequinone	0.1	7.4	74
1-Phenyl-1,2-propanedione	0.1	5.3	53
BFAM ^a	0.1	2.5	25
Isatin	0.3	6.3	21
2,3-Heptanedione	0.4	8.8	22
3,4-Hexanedione	1.6	3.9	2.4
Diacetyl	2.5	4.8	1.9
Other α-dicarbonyls			
Methylglyoxal	9.0	3.8	0.42
Glyoxal	33	0.89	0.027
3-Deoxyglucosone	37	0.96	0.026
β- and γ-Diketones			
2,5-Hexanedione	33	2.4	0.073
2,4-Pentanedione	205	3.4	0.017

^a Benzoylformic acid methyl ester.

Table 7
Kinetic constants for aldehydes and monosaccharides in the NADPH-linked reduction.

Substrate	K_m (μM)	k_{cat} (min^{-1})	k_{cat}/K_m ($\text{min}^{-1}\mu\text{M}^{-1}$)
Aromatic aldehydes			
4-Nitrobenzaldehyde	0.5	4.1	8.2
Benzaldehyde	0.7	2.6	3.7
Pyridine-3-aldehyde	5.4	6.5	1.2
Furfural	44	3.9	0.089
Alkanals			
1-Decanal	0.6	5.0	8.3
1-Nonanal	0.5	2.8	5.6
1-Heptanal	0.6	3.2	5.3
Alkenals			
4-Oxo-2-nonenal	0.3	6.1	20
Geranylgeranial	0.4	2.7	6.8
trans-2-Decenal	0.8	5.2	6.5
trans-2-Nonenal	0.5	2.5	5.0
4-Hydroxy-2-nonenal	0.3	1.3	4.3
Farnesal	1.0	3.9	3.9
4-Hydroxy-2-hexenal	1.0	0.94	0.94
trans-2-Hexenal	9.8	3.7	0.38
Crotonaldehyde	5.2	1.4	0.27
all-trans-Retinal	5.4	0.86	0.16
Acrolein	30	3.4	0.11
Monosaccharides			
L-Threose	10	1.7	0.17
L-Glyceraldehyde	49	3.6	0.073
Dihydroxyacetone	29	1.4	0.048
D-Glyceraldehyde	93	2.3	0.025
D-Threose	64	1.4	0.022
L-Erythrulose	138	2.9	0.021

ketosteroids, 5 β -dihydro-C₁₉-steroids were more efficiently reduced than their 5 α -isomers. This tendency was observed in the reduction of androstane-3,17-diones, and 4-androstene-3,17-dione was reduced with the lowest k_{cat}/K_m value. The reduction of the 3,17-diketosteroids yielded only their 17 β -ol metabolites, suggesting that AKR1C29 exclusively reduces the 17-keto group of the 3,17-diketosteroids. In contrast to the specificity in the reduction of 3- and 17-ketosteroids, Δ^4 -unsaturated, 5 α -dihydro and 5 β -dihydro forms of 20-keto-C₂₁-steroids were reduced with similar k_{cat}/K_m values, although the values for the steroids with 21-hydroxy group were higher. The reduced product of progesterone was identified as 4-pregnen-20 α -ol-3-one.

p-Quinones were efficient substrates, showing high k_{cat}/K_m values comparable to those for (S)-1-tetralol and α -3HB (Table 5).

Almost equal amounts of 4(*S*)- and 4(*R*)-TBEHs were formed in the reduction of the favorable substrate, TBE. AKR1C29 reduced 3OB and several drug ketones, although no significant activity toward ketotifen, metyrapone and acetohexamide was observed. In the reduction of 3OB both α - and β -3HBs were detected as the products, and both 6 α - and 6 β -naloxols were formed in the reduction of naloxone. The enzyme also reduced other aromatic, alicyclic and aliphatic ketones including PGD₂, acetone (3-hydroxy-2-butanone) and acetol (1-hydroxyacetone) with low K_m values of less than 56 μ M. The reduced product of PGD₂ was identified as 9 α ,11 β -PGF₂. It should be noted that no significant reductase activity toward 100- μ M PGA₂, 13,14-dihydro-15-keto-PGD₂ and PGE₂ was observed.

AKR1C29 efficiently reduced α -diketones including endogenous isatin and diacetyl, of which those with aromatic and alicyclic rings were the best substrates, showing high k_{cat}/K_m values of more than 20 min⁻¹ μ M⁻¹ (Table 6). AKR1C29 also reduced other α -dicarbonyls with an aldehyde and keto or aldehyde group, in which methylglyoxal showed high catalytic efficiency compared with 3-deoxyglucosone and glyoxal. Furthermore, 2,5-hexanedione and 2,4-pentanedione, which do not have the conjugated dicarbonyl structure, were reduced with moderate k_{cat} values (2.4 and 3.4 min⁻¹, respectively) by the enzyme.

Aromatic and lipid-derived aliphatic aldehydes were excellent substrates, as evidenced by K_m values in the micromolar or submicromolar range (Table 7). Within a series of linear alkanals and alkenals with one double bond, the catalytic efficiency tended to increase with increasing chain lengths. In the 9-carbon alkenals, the k_{cat} value for 4-oxo-2-nonenal was higher than those for 4-hydroxy-2-nonenal and 2-nonenal, suggesting that the presence of a keto group at position 4 affects the catalytic activity of AKR1C29. The enzyme efficiently reduced geranylgeranial and farnesal with more than three double bonds and branched methyl groups, but showed low reactivity to all-*trans*-retinal with a trimethylcyclohexene ring. The reduced product of farnesal was identified as farnesol. Furthermore, the enzyme reduced short-chain aldoses and ketoses, of which *L*-threose and *L*-glyceraldehyde were better

substrates than their *D*-epimers. No activity could be detected with 20-mM pentoses (*L*- and *D*-xyloses and *L*-arabinose) and hexoses (*D*-glucose, *D*-fructose and *D*-glucuronic acid) as the substrates.

3.4. Metabolism of 3OB, 17-ketosteroid and 4-oxo-2-nonenal in cells overexpressing AKR1C29

The substrate specificity for alcohols (Table 3) and carbonyl compounds (Tables 4, 5 and 7) showed that AKR1C29 catalyzes the reversible oxidation of several substrates such as 3HB and 5 β -androstan-3 α ,17 β -diol, although many nonsteroidal carbonyl compounds were irreversibly reduced. To elucidate the reaction directionality of the enzyme in the intact cells, the oxidation of α -3HB and reduction of 3OB in the AKR1C29-overexpressed BAECs were examined. The expression of cytosolic AKR1C29 in the cells transfected with the vector harboring its cDNA was confirmed by assay of (*S*)-1-tetralol dehydrogenase activity: The NADP⁺-linked activity in the cell extract was 0.038 unit/mg, in contrast to much lower activity (0.003 unit/mg) in the extract of the control BAECs, which were transfected with the vector alone. While the formation of 3OB was not observed in the incubation of the AKR1C29-overexpressed cells with α -3HB for 12 h, α -3HB and β -3HB were formed in the incubation with 3OB and their amounts were inversely correlated with the decrease in 3OB (Fig. 4A). In addition, the AKR1C29-overexpressed cells proceeded the reduction of 5 β -androstan-3 α -ol-17-one into 5 β -androstan-3 α ,17 β -diol (Fig. 4B), but not the reverse oxidation of 5 β -androstan-3 α ,17 β -diol into 5 β -androstan-3 α -ol-17-one during 12 h-incubation with the substrate. No reduced products of both 3OB and 5 β -androstan-3 α -ol-17-one were formed in the control cells (data not shown). Furthermore, we examined the protective effect of AKR1C29 against cytotoxicity of 4-oxo-2-nonenal toward BAECs, because 4-oxo-2-nonenal, the excellent substrate for the enzyme, is highly cytotoxic toward cultured cells [31]. The control cells were killed by 4-oxo-2-nonenal in a dose-dependent manner (Fig. 4C). The toxicity against the cells was attenuated by the overexpression of AKR1C29 at 4-oxo-2-nonenal concentrations of higher than 15 μ M.

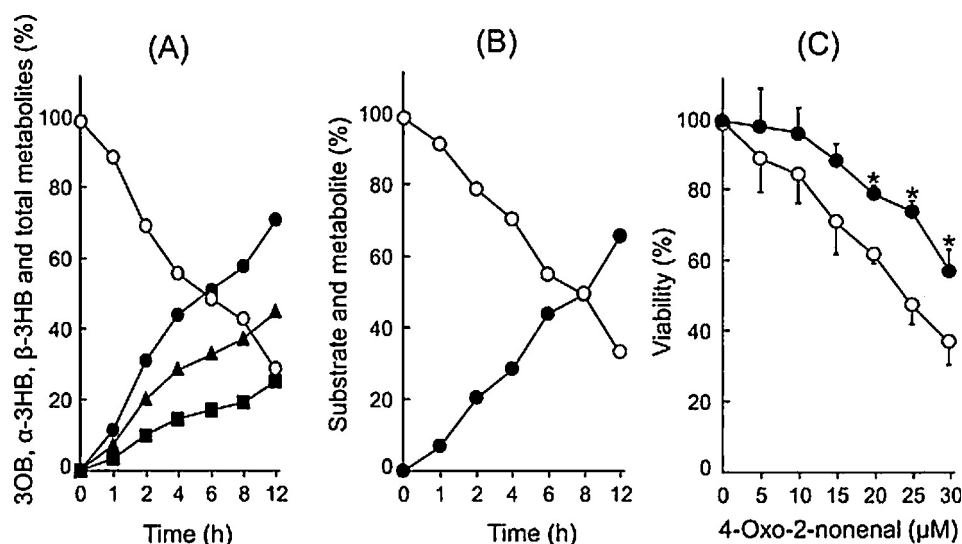


Fig. 4. Metabolism of 3OB, 5 β -androstan-3 α -ol-17-one and 4-oxo-2-nonenal in AKR1C29-overexpressed BAECs. (A) Reduction of 3OB. The cells were incubated with 0.2-mM 3OB, and a portion of the medium was taken at indicated times for determination of 3OB (\circ) and its reduced metabolites, α -3HB (\blacktriangle) and β -3HB (\blacksquare) by LC-ESI-MS. The amount of 3OB represents the remaining percentage, and those of α -3HB, β -3HB and their sum (\bullet) are expressed as the metabolic percentages, relative to the sum of 3OB and the two metabolites. Values are the means of duplicate experiments. (B) Reduction of 0.1-mM 5 β -androstan-3 α -ol-17-one. The medium was taken at indicated times for determination of 5 β -androstan-3 α -ol-17-one (\circ) and its reduced metabolite, 5 β -androstan-3 α ,17 β -diol (\bullet). The amounts of the substrate and metabolite are expressed as the remaining and metabolite percentages, respectively, as described in (A). Values are the means of duplicate experiments. (C) Protective effect of AKR1C29-overexpression against 4-oxo-2-nonenal-induced cytotoxicity. BAECs were transfected for 48 h with the expression vector alone (control, \circ) and the vector carrying AKR1C29 cDNA (overexpressing, \bullet), and then treated for 24 h with various concentrations of 4-oxo-2-nonenal. The viability is shown as the mean \pm SD, evaluated by using the unpaired Student's *t*-test and ANOVA followed by Fisher's test, $n = 3$. *Significant difference ($p < 0.05$) from the control cells.

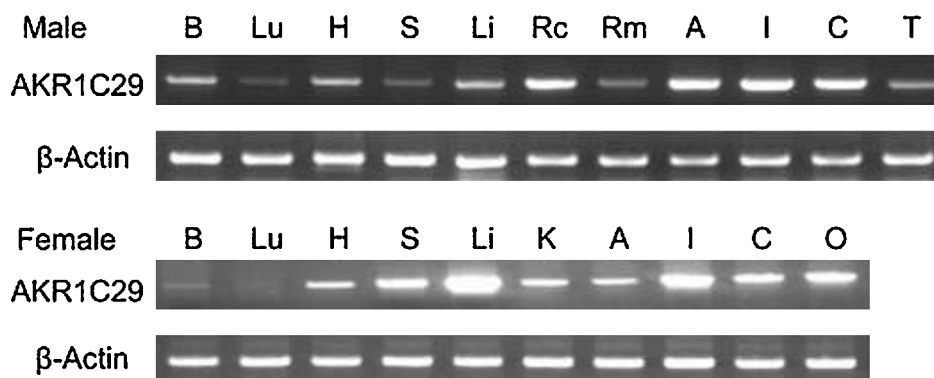


Fig. 5. RT-PCR analysis for expression of mRNA for AKR1C29 in tissues of male and female rabbits. Tissues: brain (B), lung (Lu), heart (H), stomach (S), liver (Li), adrenal gland (A), small intestine (I), colon (C), testis (T) and ovary (O). The kidney of the male rabbit was divided into the renal cortex (Rc) and renal medulla (Rm), while whole kidney (K) of female rabbit was used. The expression of mRNA for β -actin is shown as the control.

3.5. Inhibitor sensitivity

The β -ionol dehydrogenase activity of AKR1C29 was inhibited by phenolphthalein ($IC_{50} = 3.4 \mu\text{M}$), but it was not affected by 50- μM phenolphthalin (an open form of the phthalein ring), 4,5,6,7-tetrabromophthalein or 3',3'',5',5''-tetrabromophthalein. The enzyme activity was also inhibited by nonsteroidal anti-inflammatory drugs such as tolafenamic acid, mefenamic acid and flufenamic acid (IC_{50} values of 8.8, 22 and 39 μM , respectively), synthetic estrogens such as hexestrol, diethylstilbestrol and dienestrol (IC_{50} values of 27, 31 and 38 μM , respectively), and flavonoids such as kaempferol, 7-hydroxyflavone and quercetin (IC_{50} values of 12, 17 and 22 μM , respectively). The inhibition patterns of phenolphthalein and tolafenamic acid were competitive with respect to β -ionol, and their K_i values were 0.82 and 1.2 μM , respectively. No significant inhibition (less than 25%) was observed with 10- μM medroxyprogesterone acetate, 50- μM steroidal anti-inflammatory drugs (dexamethasone, betamethasone and 6 α -methylprednisolone), bile acids (isolithocholic acid and lithocholic acid), glycyrrhetic acid and 1-mM 1,10-phenanthroline, which inhibit HSDs [32,33] of the AKR1C subfamily. The enzyme was also not inhibited by known inhibitors of aldehyde reductase (1-mM valproic acid, barbital and diphenic acid) [34] and a rabbit dihydrodiol dehydrogenase isoform, CM-2 (1-mM phenobarbital) [15].

3.6. Tissue distribution

The tissue distribution of AKR1C29 was assessed by RT-PCR (Fig. 5). The expression level of the mRNA for the enzyme was high in the kidney, adrenal gland, intestine and colon of male rabbits, and low in the other tissues. The mRNA was expressed more highly in the cortex than the medulla of rabbit kidney. Similar expression pattern of the transcript in female rabbit tissues was observed, except that the expression levels in the stomach and liver were higher compared to male rabbits.

4. Discussion

This report describes the cloning and characterization of rabbit 3HBD that has been thought to act as a dehydrogenase [5–7]. The enzyme is a member (AKR1C29) of the AKR superfamily, and efficiently reduced carbonyls derived from a broad range of structural classes, including both aromatic and aliphatic aldehydes and ketones, using NADPH as the preferred coenzyme. The preference for NADP(H) is evidenced by the high k_{cat}/K_m values for NADP(H) compared with those for NAD(H) and the potent inhibition of the NAD(H)-linked activities by NADP(H), in which the affinity for NADPH (indicated by the K_i value) was significantly

high. In addition to the high cellular ratio of NADPH/NADP⁺ [35,36], the high affinity for NADPH suggests that AKR1C29 primarily acts as a reductase. The directional preferences of HSDs in the cells are reported to be governed by relative affinities for NAD(P)(H) and existing coenzyme gradients [36]. The data using the AKR1C29-overexpressed cells demonstrated that the intracellular enzyme catalyzes the reduction of both 3OB and 5 β -androstan-3 α -ol-17-one, but not the reverse reactions. Therefore, we concluded that AKR1C29 acts as an NADPH-dependent reductase. This raises the question of what enzyme(s) are responsible for the metabolism of 3HB into 3OB in the rabbit. With respect to the cellular coenzyme gradients, NAD⁺-dependent dehydrogenases may act as the 3HBD. NAD⁺-dependent AKRs of rats (AKR1C24) [37] and mice (AKR1C19) [38] have been reported to oxidize α -3HB and β -3HB. We identified three rabbit orthologs of AKR1C24 (AKR1C26, AKR1C27 and AKR1C28) [16], of which AKR1C26 and AKR1C28 oxidized α -3HB more efficiently than β -3HB, showing K_m values of 7.6 and 7.0 μM , respectively, and k_{cat} values of 1.2 and 7.2 min^{-1} , respectively, at pH 7.4 and 25 °C. The two rabbit NAD⁺-dependent dehydrogenases may function in the metabolism of 3HB into 3OB. AKR1C29 shows 74% overall amino acid sequence identity with hamster 3HBD [11], but between the two enzymes there is no difference in the coenzyme-binding residues (Fig. 2) that are shown by crystallographic studies of other AKRs [33,39–42]. Hamster 3HBD shows higher V_{max}/K_m value for NADP⁺ than NAD⁺ even at its optimal pH of 8.5 [11], and might also act as a reductase using NADPH as the coenzyme under physiological conditions.

The newly found alcohol substrates of AKR1C29 include *trans*-benzene dihydrodiol, which is a representative substrate of dihydrodiol dehydrogenase [15]. Monomeric AKR1C29 differs from the tetrameric and dimeric forms of rabbit dihydrodiol dehydrogenase purified by Klein et al. [15]. Another monomeric rabbit enzyme with *trans*-benzene dihydrodiol dehydrogenase activity is indanol dehydrogenase, which exists in seven multiple forms associated with 3 α -HSD and/or 17 β -HSD activities [12]. Among the seven forms (A1–A7), A6 is the most similar to AKR1C29 in its pH optima of the NAD⁺- and NADP⁺-linked activities, low K_m values for 1-acenaphthenol and 1-indanol, and sensitivity to the three synthetic estrogens and flufenamic acid.

Other endogenous alcohol substrates of AKR1C29 found in this study are some 3 α - and 20 α -hydroxysteroids, in addition to 17 β -hydroxysteroids that were previously reported [7]. AKR1C29 is different from hamster 3HBD [11] in its inability to oxidize bile acids and exhibiting 20 α -HSD activity, which may result from differences in the substrate-binding residues (positions 54, 128, 306, 310 and 311, Fig. 2) between the two enzymes. In contrast to its low k_{cat}/K_m values for the hydroxysteroids, AKR1C29 efficiently reduced various 3-, 17- and 20-ketosteroids in the reverse reaction.

The product identification of the ketosteroid reduction indicates that AKR1C29 is a reductive $3\alpha/17\beta/20\alpha$ -HSD. Because it did not oxidize 17β -estradiol, AKR1C29 may be distinct from multiple forms of NADP⁺-dependent 17β -HSD purified from female rabbit liver [13]. The broad steroid specificity of AKR1C29 and its sensitivity to hexestrol resemble the properties of rabbit $3\alpha/3\beta/17\beta/20\alpha$ -HSD [14], although the $3\alpha/3\beta/17\beta/20\alpha$ -HSD substrate, 5α -androstan- 3β -ol-17-one, was slightly oxidized by AKR1C29. AKR1C29 shows the highest sequence identity with rabbit 20α -HSD (AKR1C5) [43] among the known AKRs. AKR1C5 is specifically expressed in ovary and uterus of female rabbits [43,44] and reduces progesterone, estrone, dehydroepiandrosterone [40,45] and PGE₂ [44], an indication of its major role in the termination of pregnancy by both inactivation of progesterone and synthesis of 17β -estradiol and PGF_{2 α} . AKR1C29 differs from AKR1C5 in its inability to reduce estrone, dehydroepiandrosterone and PGE₂, and its low sensitivity to the inhibition by phenolphthalein, its derivatives and flavonoids compared with that of AKR1C5 [45], in addition to its ubiquitous expression in tissues of both male and female rabbits. Therefore, AKR1C29 may play a pivotal role in controlling the concentrations of cellular androgen (5α -androstan- 17β -ol-3-one), progesterone and neuroactive steroids (5α -pregnan- 3α -ol-20-one and 5α -pregnane- $3\alpha,21$ -diol-20-one) in rabbit tissues other than the ovary and uterus, in addition to hepatic metabolism of ketosteroids.

Several cytosolic, monomeric (28–35 kDa) and NADPH-dependent drug ketone reductases with HSD activity were purified from rabbit livers. They are loxoprofen reductase with 3-ketosteroid reductase activity [46], befunolol reductase with 3α -HSD activity [47], and two naloxone reductases with 3α -HSD or 17β -HSD activity [48]. AKR1C29 reduced the three drugs, but its sequence is clearly different from the befunolol reductase [49] and naloxone reductases [48]. Additionally, its broad specificity for 3-, 17- and 20-ketosteroids is distinct from the specificity of loxoprofen reductase confined to 3-ketosteroids [46]. In the purification of the reductases for loxoprofen [46] and naloxone [48] other multiple enzyme forms were found, and more than five multiple forms of rabbit reductase for naloxone, naltrexone and/or daunorubicin have been separated [50]. AKR1C29 probably corresponds to one of these uncharacterized multiple forms of the drug ketone reductase(s), and may act as an efficient reductase toward loxoprofen, naloxone, daunorubicin and befunolol because of its lower K_m values compared to those of the above known drug ketone reductases.

AKR1C29 represents a unique member of the AKR superfamily with respect to its extremely broad substrate specificity and low K_m values, and is ubiquitously distributed in rabbit tissues. Based on the broad substrate specificity of the enzyme and tissue distribution, the following physiological roles in metabolism of endogenous carbonyl compounds could be considered. (1) Reduction of PGD₂: A 66-kDa PGD₂ 11-ketoreductase was purified from rabbit liver cytosol [51], while the 36-kDa enzymes belonging to the AKR superfamily were purified or cloned from bovine lung [28] and liver [52], and human tissues [53]. The K_m value (4 μ M) of AKR1C29 is comparable to those (3.4–10 μ M) of the bovine and human enzymes, but is much lower than 200 μ M of the 66-kDa rabbit enzyme [51]. AKR1C29 may be involved in the metabolism of PGD₂ in many rabbit tissues, although further comparative studies of the two rabbit enzymes are needed with respect to their tissue expression and ability to catalyze the conversion of PGH₂ into PGF_{2 α} that is associated in the human and bovine enzymes. (2) Detoxification of reactive endogenous carbonyl compounds, which include the lipid-derived long-chain aldehydes [18,31,54] and α -dicarbonyl compounds such as methylglyoxal, glyoxal and 3-deoxyglucosone that are related to glycation [55]. These reactive carbonyl compounds are substrates of rabbit aldose reductase

(AKR1B2), its similar enzyme (AKR1B19) [25] and AKR1C5 [45], in addition to AKR1C29. Among the rabbit enzymes, AKR1C29 shows the highest k_{cat}/K_m values for most alkenals including highly reactive 4-oxo-2-nonenal and 4-hydroxy-2-nonenal. This efficiency in the cells is demonstrated by the protective effect of AKR1C29 overexpression against the cytotoxicity of 4-oxo-2-nonenal. The k_{cat}/K_m value for methylglyoxal of AKR1C29 is comparable to that of AKR1B2, and superior to those of AKR1B19 and AKR1C5. The k_{cat}/K_m value for glyoxal is higher than those of AKR1B2 and AKR1B19 (0.009 and 0.002 min⁻¹ μ M⁻¹, respectively), although the value for 3-deoxyglucosone is lower than that of AKR1B2. AKR1C29 reduced another reactive dicarbonyl compound, diacetyl, more efficiently than the other rabbit AKRs, and also reduced acetoin, the reduced product of diacetyl. AKR1C29 appears to function as a defense system against these naturally occurring reactive carbonyl compounds in many rabbit tissue cells. (3) Metabolism of isatin and monosaccharides. Isatin is an endogenous monoamine oxidase inhibitor [56] and antagonist of atrial natriuretic peptide function and nitric oxide signaling [57]. It is one of the best endogenous substrates of AKR1C29, showing much higher k_{cat}/K_m value than those of the above other AKRs in rabbits. AKR1C29 may be involved in controlling the intracellular concentration of the biologically active isatin. In addition, AKR1C29 reduced short-chain aldoses, of which trioses and tetroses generate superoxide anions in glycation reactions [58] and L-threose, one of the oxidation products of ascorbic acid, is suggested to be a potent glycation agent [59]. Although no rabbit reductase for L-threose has been reported, the K_m value for L-threose of AKR1C29 is much lower than those (350–750 μ M) of human aldose reductase (AKR1B1) [60], rat aldose reductase-like (AKR1B18) [61] and rat AKR1C15 [62]. This ability to reduce the short-chain aldoses may also contribute to prevention of the progress of glycation in rabbits.

Conflict of interest

None declared.

Acknowledgements

This work was partly founded by grant-in-aid for Young Scientists (B) from the Japan Society for the Promotion of Science, and by a Sasakawa Scientific Research Grant from Japan Science Society.

References

- [1] Knodell RG, Dubeck RK, Wilkinson GR, Guengerich FP. Oxidative metabolism of hexobarbital in human liver: relationship to polymorphic S-mephenytoin 4-hydroxylation. *J Pharmacol Exp Ther* 1988;245:845–9.
- [2] Takenoshita R, Toki S. New aspects of hexobarbital metabolism: stereoselective metabolism, new metabolic pathway via GSH conjugation, and 3-hydroxyhexobarbital dehydrogenases. *Yakugaku Zasshi* 2004;124:857–71.
- [3] Miyano K, Ota T, Toki S. Stereoselective formation of glucuronides in metabolism of hexobarbital enantiomers in vivo: isolation and quantitation of glucuronides in rabbit urine. *Drug Metab Dispos* 1981;9:60–4.
- [4] Takenoshita R, Nakamura T, Toki S. Hexobarbital metabolism: a new metabolic pathway to produce 1,5-dimethylbarbituric acid and cyclohexenone-glutathione adduct via 3'-oxohexobarbital. *Xenobiotica* 1993;23:925–34.
- [5] Takenoshita R, Toki S. Rabbit liver 3-hydroxyhexobarbital dehydrogenase. Purification and properties. *J Biol Chem* 1974;249:5428–9.
- [6] Takenoshita R, Toki S. Dehydrogenation of indanol by rabbit liver 3-hydroxyhexobarbital dehydrogenase. *Xenobiotica* 1977;7:383–91.
- [7] Takenoshita R, Toki S. 5β -Androstane- $3\alpha,17\beta$ -diol: an endogenous substrate for rabbit liver 3-hydroxyhexobarbital dehydrogenase. *Biochem Pharmacol* 1978;27:989–93.
- [8] Kageura E, Toki S. Guinea pig liver 3-hydroxyhexobarbital dehydrogenase as a 17β -hydroxysteroid dehydrogenase. *Biochim Biophys Acta* 1974;341:172–7.
- [9] Kageura E, Toki S. Guinea pig liver 3-hydroxyhexobarbital dehydrogenase. Purification and properties. *J Biol Chem* 1975;250:5015–9.
- [10] Takenoshita R, Naitoh K, Toki S. Mouse liver 3-hydroxyhexobarbital dehydrogenase: purification and substrate specificity. *Prog Clin Biol Res* 1989;290:279–91.

- [11] Takenoshita R, Nomura Y, Toki S. Cloning and expression of cDNA encoding hamster liver 3-hydroxyhexobarbital/17 β (3 α)-hydroxysteroid dehydrogenase 1. *Chem Biol Interact* 2001;130–132:863–70.
- [12] Hara A, Kariya K, Nakamura M, Nakayama T, Sawada H. Isolation of multiple forms of indanol dehydrogenase associated with 17 β -hydroxysteroid dehydrogenase activity from male rabbit liver. *Arch Biochem Biophys* 1986;249:225–36.
- [13] Antoun GR, Brglez I, Williamson DG. A 17 β -hydroxysteroid dehydrogenase of female rabbit liver cytosol. Purification and characterization of multiple forms of the enzyme. *Biochem J* 1985;225:383–90.
- [14] Smirnov AN. Estrophilic 3 α ,3 β ,17 β ,20 α -hydroxysteroid dehydrogenase from rabbit liver-I. Isolation and purification. *J Steroid Biochem* 1990;36:609–16.
- [15] Klein J, Thomas H, Post K, Wörner W, Oesch F. Dihydrodiol dehydrogenase activities of rabbit liver are associated with hydroxysteroid dehydrogenases and aldo-keto reductases. *Eur J Biochem* 1992;205:1155–62.
- [16] Endo S, Matsunaga T, Fujimoto A, Kumada S, Arai Y, Miura Y, et al. Characterization of rabbit morphine 6-dehydrogenase and two NAD⁺-dependent 3 α (17 β)-hydroxysteroid dehydrogenases. *Arch Biochem Biophys* 2013;529:131–9.
- [17] Platt K, Oesch F. An improved synthesis of *trans*-5,6-dihydroxy-1,3-cyclohexadiene (*trans*-1,2-dihydroxy-1,2-dihydrobenzene). *Synthesis* 1977;7:449–50.
- [18] Doorn JA, Srivastava SK, Petersen DR. Aldose reductase catalyzes reduction of the lipid peroxidation product 4-oxonon-2-enal. *Chem Res Toxicol* 2003;16:1418–23.
- [19] Doyle MP, Yan M. Attempted synthesis of casbene by intramolecular cyclopropanation. *ARKIVOC* 2002;viii:180–5.
- [20] Cone EJ, Gorodetzky CW, Yeh SY. Biosynthesis, isolation and identification of 6 β -hydroxynaltrexone, a major human metabolite of naltrexone. *J Pharm Sci* 1975;64:618–21.
- [21] Chatterjee N, Inturrisi CE. Stereospecific synthesis of the 6 β -hydroxy metabolites of naltrexone and naloxone. *J Med Chem* 1975;18:490–2.
- [22] Tajima K, Hashizaki M, Yamamoto K, Mizutani T. Metabolism of 3-*tert*-butyl-4-hydroxyanisole by horseradish peroxidase and hydrogen peroxide. *Drug Metab Dispos* 1992;20:816–20.
- [23] Tajima K, Hashizaki M, Yamamoto K, Mizutani T. Carbonyl reduction of 6-*tert*-butyl-2,3-epoxy-1,4-benzoquinone, a metabolite of 3-*tert*-butyl-4-hydroxyanisole, by rat liver microsomes and cytosol. *Drug Metab Dispos* 1994;22:815–8.
- [24] Sambrook J, Fritsch EF, Maniatis T. *Molecular Cloning: A Laboratory Manual*. 2nd ed. Cold Spring Harbor: Cold Spring Harbor Laboratory; 1989.
- [25] Endo S, Matsunaga T, Kumada S, Fujimoto A, Ohno S, El-Kabbani O, et al. Characterization of rabbit aldose reductase-like protein with 3 β -hydroxysteroid dehydrogenase activity. *Arch Biochem Biophys* 2012;527:23–30.
- [26] Ohno S, Matsui M, Yokogawa T, Nakamura M, Hosoya T, Hiramatsu T, et al. Site-specific post-translational modification of proteins using an unnatural amino acid, 3-azidotyrosine. *J Biochem* 2007;141:335–43.
- [27] Parés X, Julià P. Isoenzymes of alcohol dehydrogenase in retinoid metabolism. *Methods Enzymol* 1990;189:436–41.
- [28] Watanabe K, Iguchi Y, Iguchi S, Arai Y, Hayaishi O, Roberts II LJ. Stereospecific conversion of prostaglandin D₂ to (5Z,13E)-(15S)-9 α ,-11 β ,15-trihydroxyprosta-5,13-dien-1-oic acid (9 α ,11 β -prostaglandin F₂) and of prostaglandin H₂ to prostaglandin F_{2 α} , by bovine lung prostaglandin F synthase. *Proc Natl Acad Sci USA* 1986;83:1583–7.
- [29] Endo S, Matsunaga T, Ohta C, Soda M, Kanamori A, Kitade Y, et al. Roles of rat and human aldo-keto reductases in metabolism of farnesol and geranylgeraniol. *Chem Biol Interact* 2011;191:261–8.
- [30] Tanaka N, Aoki K, Ishikura S, Nagano M, Imamura Y, Hara A, et al. Molecular basis for peroxisomal localization of tetrameric carbonyl reductase. *Structure* 2008;16:388–97.
- [31] Shibata T, Iio K, Kawai Y, Shibata N, Kawaguchi M, Toi S, et al. Identification of a lipid peroxidation product as a potential trigger of the p53 pathway. *J Biol Chem* 2006;281:1196–204.
- [32] Higaki Y, Usami N, Shintani S, Ishikura S, El-Kabbani O, Hara A. Selective and potent inhibitors of human 20 α -hydroxysteroid dehydrogenase (AKR1C1) that metabolizes neurosteroids derived from progesterone. *Chem Biol Interact* 2003;143–144:503–13.
- [33] Byrns MC, Jin Y, Penning TM. Inhibitors of type 5 17 β -hydroxysteroid dehydrogenase (AKR1C3): overview and structural insights. *J Steroid Biochem Mol Biol* 2011;125:95–104.
- [34] Kanazu T, Shinoda M, Nakayama T, Deyashiki Y, Hara A, Sawada H. Aldehyde reductase is a major protein associated with 3-deoxyglucosone reductase activity in rat, pig and human livers. *Biochem J* 1991;279:903–6.
- [35] Veech RL, Eggleston LV, Krebs HA. The redox state of free nicotinamide adenine dinucleotide phosphate in the cytoplasm of rat liver. *Biochem J* 1969;115:609–19.
- [36] Sherbet DP, Papari-Zareei M, Khan N, Sharma KK, Brandmaier A, Rambally S, et al. Cofactors, redox state, and directional preferences of hydroxysteroid dehydrogenases. *Mol Cell Endocrinol* 2007;265–266:83–8.
- [37] Ishikura S, Matsumoto K, Sanai M, Horie K, Matsunaga T, Tajima K, et al. Molecular cloning of a novel type of rat cytoplasmic 17 β -hydroxysteroid dehydrogenase distinct from the type 5 isozyme. *J Biochem* 2006;139:1053–63.
- [38] Ishikura S, Horie K, Sanai M, Matsumoto K, Hara A. Enzymatic properties of a member (AKR1C19) of the aldo-keto reductase family. *Biol Pharm Bull* 2005;28:1075–8.
- [39] Jez JM, Bennett MJ, Schlegel BP, Lewis M, Penning TM. Comparative anatomy of the aldo-keto reductase superfamily. *Biochem J* 1997;326:625–36.
- [40] Couture JF, Legrand P, Cantin L, Labrie F, Luu-The V, Breton R. Loop relaxation, a mechanism that explains the reduced specificity of rabbit 20 α -hydroxysteroid dehydrogenase, a member of the aldo-keto reductase superfamily. *J Mol Biol* 2004;339:89–102.
- [41] Sanli G, Dudley JJ, Blaber M. Structural biology of the aldo-keto reductase family of enzymes: catalysis and cofactor binding. *Cell Biochem Biophys* 2003;38:79–101.
- [42] Penning TM. Molecular determinants of steroid recognition and catalysis in aldo-keto reductases. Lessons from 3 α -hydroxysteroid dehydrogenase. *J Steroid Biochem Mol Biol* 1999;69:211–25.
- [43] Lacy WR, Washenick KJ, Cook RG, Dunbar BS. Molecular cloning and expression of an abundant rabbit ovarian protein with 20 α -hydroxysteroid dehydrogenase activity. *Mol Endocrinol* 1993;7:58–66.
- [44] Wintergalen N, Thole HH, Galla HJ, Schlegel W. Prostaglandin E₂ 9-reductase from corpus luteum of pseudopregnant rabbit is a member of the aldo-keto reductase superfamily featuring 20 α -hydroxysteroid dehydrogenase activity. *Eur J Biochem* 1995;234:264–70.
- [45] Endo S, Arai Y, Hara A, Kitade Y, Bunai Y, El-Kabbani O, et al. Substrate specificity and inhibitor sensitivity of rabbit 20 α -hydroxysteroid dehydrogenase. *Biol Pharm Bull* 2013;36:1514–8.
- [46] Tanaka Y, Nishikawa Y, Matsuda K, Yamazaki M, Hayashi R. Purification and some properties of ketone reductase forming an active metabolite of sodium 2-[4-(2-oxocyclopentylmethyl)-phenyl]propionate dihydrate (loxoprofen sodium), a new anti-inflammatory agent, in rabbit liver cytosol. *Chem Pharm Bull (Tokyo)* 1984;32:1040–8.
- [47] Imamura Y, Nozaki Y, Otagiri M. Purification and characterization of befunolol reductase from rabbit liver. *Chem Pharm Bull (Tokyo)* 1989;37:3338–42.
- [48] Yamano S, Ichinose F, Todaka T, Toki S. Purification and characterization of two major forms of naloxone reductase from rabbit liver cytosol, new members of aldo-keto reductase superfamily. *Biol Pharm Bull* 1999;22:1038–46.
- [49] Imamura Y, Koga T, Otagiri M, Satoh K, Hara A. Carbonyl reductase purified from rabbit liver is not the product of a carbonyl reductase gene (RCBR5 or RCBR6) cloned from the rabbit liver cDNA library. *Biol Pharm Bull* 1998;21:76–8.
- [50] Felsted RL, Richter DR, Jones DM, Bachur NR. Isolation and characterization of rabbit liver xenobiotic carbonyl reductases. *Biochem Pharmacol* 1980;29:1503–16.
- [51] Wong PY. Purification and partial characterization of prostaglandin D₂ 11-keto reductase in rabbit liver. *Biochim Biophys Acta* 1981;659:169–78.
- [52] Suzuki T, Fujii Y, Miyano M, Chen LY, Takahashi T, Watanabe K. cDNA cloning, expression, and mutagenesis study of liver-type prostaglandin F synthase. *J Biol Chem* 1999;274:241–8.
- [53] Suzuki-Yamamoto T, Nishizawa M, Fukui M, Okuda-Ashitaka E, Nakajima T, Ito S, Watanabe K. cDNA cloning expression and characterization of human prostaglandin synthase. *FEBS Lett* 1999;462:335–40.
- [54] Esterbauer H, Schaur RJ, Zollner H. Chemistry and biochemistry of 4-hydroxynonenal, malonaldehyde and related aldehydes. *Free Radic Biol Med* 1991;11:81–128.
- [55] Kroh LW, Fiedler T, Wagner J. α -Dicarbonyl compounds—key intermediates for the formation of carbohydrate-based melanoidins. *Ann N Y Acad Sci* 2008;1126:210–5.
- [56] Igosheva N, Lorz C, O'Conner E, Glover V, Mehmet H. Isatin, an endogenous monoamine oxidase inhibitor, triggers a dose- and time-dependent switch from apoptosis to necrosis in human neuroblastoma cells. *Neurochem Int* 2005;47:216–24.
- [57] Medvedev A, Igosheva N, Crumeyrolle-Arias M, Glover V. Isatin: role in stress and anxiety. *Stress* 2005;8:175–83.
- [58] Ortwerth BJ, Speaker JA, Prabhakaram M, Lopez MG, Li EY, Feather MS. Ascorbic acid glycation: the reactions of L-threose in lens tissue. *Exp Eye Res* 1994;58:665–74.
- [59] Ortwerth BJ, James H, Simpson G, Linetsky M. The generation of superoxide anions in glycation reactions with sugars, osones, and 3-deoxyosones. *Biochem Biophys Res Commun* 1998;245:161–5.
- [60] Devamanoharan PS, Varma SD. Studies on L-threose as substrate for aldose reductase: a possible role in preventing protein glycation. *Mol Cell Biochem* 1996;159:123–7.
- [61] Endo S, Matsunaga T, Kuragano T, Ohno S, Kitade Y, Tajima K, et al. Properties and tissue distribution of a novel aldo-keto reductase encoding in a rat gene (*Akr1b10*). *Arch Biochem Biophys* 2010;503:230–7.
- [62] Endo S, Matsunaga T, Horie K, Tajima K, Bunai Y, Carbone V, et al. Enzymatic characteristics of an aldo-keto reductase family protein (AKR1C15) and its localization in rat tissues. *Arch Biochem Biophys* 2007;465:136–47.